

BiFold: A Python code for the calculation of double folded (bifold) potentials with density-in/dependent nucleon-nucleon interactions

Mesut Karakoç*

*Department of Physics, Faculty of Science,
Akdeniz University, TR 07070, Antalya, Turkey*

Abstract

BiFold calculates the density-dependent (DDM3Yn, BDM3Yn, CDM3Yn) or independent double folded potentials between two colliding spherical nuclei. It is written in a Python package form to give the ability to use the potentials directly in a nuclear reaction/structure code. In addition to using Woods-Saxon/Fermi or Gaussian functions, the code also allows for the definition of nuclear matter densities using pre-calculated densities in a data file. The manuscript provides an overview of the double folding model and the use of the code.

Keywords: Nuclear interaction; Double folded potentials; Density-dependent NN interactions; M3Y-interaction.

PROGRAM SUMMARY

Program Title: BiFold

CPC Library link to program files: (to be added by Technical Editor)

Developer's repository link: <https://github.com/mkarakoc/BiFold>

Code Ocean capsule: (to be added by Technical Editor)

Licensing provisions: GPLv3

Programming language: Python 3.x

Nature of problem: BiFold calculates the real part of the nuclear potential between two colliding spherical nuclei by integrating a density-independent/dependent nucleon-nucleon (NN) interaction [1, 2, 3] over the nuclear matter densities of the two nuclei. The code based on M3Y Reid/Paris NN interactions [1, 2, 3] by default, but it is possible to define custom NN interactions when necessary.

Solution method: The code uses the Fourier transform method in spherical coordinates to calculate the potential. The method simplifies the sixfold integration [1] and makes the calculation a lot faster. The integration is done by default using Simpson's integration method, but Filon's integration method is also available.

References

- [1] G.R. Satchler and W.G. Love, Phys. Rep. 55 (1979) 183.

*Corresponding author.

E-mail address: karakoc@akdeniz.edu.tr or mesutkarakoc@gmail.com

Preprint submitted to Computer Physics Communications

September 28, 2022

- [2] A. Kobos, B. Brown, P. Hodgson, G. Satchler and A. Budzanowski, NPA 384 (1) (1982) 65–87.
 [3] D. T. Khoa, W. von Oertzen, H. G. Bohlen, S. Ohkubo, J. Phys. G: Nucl. Part. Phys. 34 (3) (2007) R111–R164.

1. Introduction

The folded potential model [1] is a well-known model for describing the mean-field nuclear interaction between two colliding nuclei. It has been widely used in the literature [1, 2, 3, 4] since accepted as a more realistic approach than a phenomenological potential such as the well-known Woods-Saxon. The latter usually needs three free parameters to fit data, and this may create possible known ambiguities [5]. On the contrary, a folded potential usually has only one free parameter called the re-normalization factor to compensate for higher-order effects in a nuclear reaction. Folded potentials have two categories single folded (SF) potentials and double folded (DF) potentials.

The SF potential describes the interaction between two nuclei using one of the two nuclei's densities and a phenomenological nucleon-nucleus interaction potential. The shortcomings of this treatment are density dependence, surface features, or couplings of a nuclear system are not well defined, as pointed out in the report [1] of Satchler and Love. These shortcomings make the depth of the SF potentials unrealistically deep [6, 2] to explain the rainbow scattering.

The usual DF potential between two spherical nuclei is constructed by integrating over an effective nucleon-nucleon (NN) interaction with nuclear matter densities representing nucleons of both nuclei. Although, DF potentials would overcome the shortcomings of SF potentials. Some cases for DF potentials can still overestimate the depth of the nuclear potential. Additionally, it is necessary to add the antisymmetrization-exchange effects and the density-dependent saturation effects in the effective NN interaction [2] for a more realistic nuclear potential.

The main reason for density dependence (DD) at NN interaction is the Pauli principle effects in the nuclear medium of both colliding nuclei. The DD of NN interaction has several treatments in the literature, but the code BiFold is built on the treatments of Satchler and Love [1], Kobos *et al.* [2], and Khoa *et al.* [3]. All these three treatments have the frozen density approximation while the case of Kobos *et al.* [2] has energy dependence, but the other two have no energy dependence.

Many studies (*see the references in the present work*) have used these DD treatments of NN interactions, but there are very few published codes [7, 8] to be able to reproduce the results of these works. In addition, the codes have limitations, and not all are updated regularly. For example, DFPOT [7] cannot calculate the potentials with the DDM3Y, BDM3Y n ($n = 1, 2, 3$), and CDM3Y n ($n = 1 \dots 6$) type density-dependent interactions [3]. While DFMSPH [8] can calculate many of those, it does not support BDM3Y2, BDM3Y3 [9], and the first version of DDM3Y [2]. And it is a well-known fact results of a study must be reproducible in science. Therefore, the code BiFold will help the community in these manners.

2. The model

2.1. The usual double folded potential

It can be claimed that Coulomb potential between two spherical charges is the inspiration for the double folded potentials. And it is formulated as [1, 4]

$$U_{DF}(\vec{R}) = \int \int d\vec{r}_p d\vec{r}_t \rho_p(\vec{r}_p) \rho_t(\vec{r}_t) v(\vec{s}), \quad (1)$$

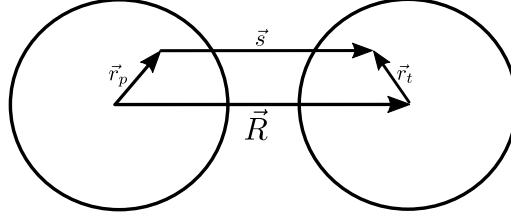


Figure 1: It is the schematic representation of DF potential in Eq. (1) where \vec{R} is the vector between the centers of the projectile (p) and the target (t) nuclei. \vec{r}_p and \vec{r}_t are the locations of the interacting parts of the nucleon distributions of both nuclei. And $\vec{s} = \vec{R} + \vec{r}_t - \vec{r}_p$ is the separation between them.

where ρ_p and ρ_t are charge densities, and $v(\vec{s}) = 1/s$ interaction between charges in Coulomb potential case, while ρ_p and ρ_t are nuclear matter densities, and $v(\vec{s})$ is the effective NN interaction between point-like nucleons in nuclear potential case. Its schematic representation and definitions of the vectors are given in Fig. 1.

The effective NN interaction $v(\vec{s})$ is density-independent in this usual definition of the DF potentials. The medium effects are included in the calculations by changing $v(\vec{s})$ with $v(\rho, \vec{s}) = F(\rho)v(\vec{s})$, where $F(\rho)$ describes the density dependence of the NN interaction.

2.2. Effective density-independent NN interactions

Although BiFold can use a wide range of density-independent NN interactions in the DF potential calculations, M3Y type interactions [10, 9, 11] are defined by default in the code since they are perhaps the most widely used ones.

These interactions are called M3Y-Reid [12] and M3Y-Paris [13] effective interactions. The former is derived from the solution of the Bethe-Goldstone equation with Reid [12] soft-core interaction on a harmonic oscillator basis to obtain G-matrix. The latter is derived from a more fundamental Paris NN potential [13] to generate all components of the effective interaction [14].

Both versions of the NN interactions have direct (v_d) and exchange (v_{ex}) parts,

M3Y-Reid:

$$v_d(\vec{s}) = \left[7999 \frac{e^{-4s}}{4s} - 2134 \frac{e^{-2.5s}}{2.5s} \right] \text{ MeV}, \quad (2)$$

$$\text{ZR: } v_{ex}(\vec{s}) = J_{ex}(E)\delta(\vec{s}) \quad \text{where} \quad J_{ex}(E) \approx -276[1 - 0.005E] \text{ MeVfm}^3, \quad (3)$$

$$\text{FR: } v_{ex}(\vec{s}) = \left[4631 \frac{e^{-4s}}{4s} - 1787 \frac{e^{-2.5s}}{2.5s} - 7.847 \frac{e^{-0.7072s}}{0.7072s} \right] \text{ MeV}, \quad (4)$$

M3Y-Paris:

$$v_d(\vec{s}) = \left[11062 \frac{e^{-4s}}{4s} - 2538 \frac{e^{-2.5s}}{2.5s} \right] \text{ MeV}, \quad (5)$$

$$\text{ZR: } v_{ex}(\vec{s}) = J_{ex}(E)\delta(\vec{s}) \quad \text{where} \quad J_{ex}(E) \approx -590[1 - 0.002E] \text{ MeVfm}^3, \quad (6)$$

$$\text{FR: } v_{ex}(\vec{s}) = \left[-1524 \frac{e^{-4s}}{4s} - 518.8 \frac{e^{-2.5s}}{2.5s} - 7.847 \frac{e^{-0.7072s}}{0.7072s} \right] \text{ MeV}, \quad (7)$$

while the direct one defines the usual nuclear interaction between nucleons. The exchange part describes the interchange (knock-on exchange) of the nucleons of the colliding nuclei [9, 11]. The DF potential will have two parts since the effective NN interactions have two parts; then Eq. (1) will have a new form

$$U_{DF}(\vec{R}) = U_D(\vec{R}) + U_{EX}(\vec{R}) = \int \int d\vec{r}_p d\vec{r}_t \rho_p(\vec{r}_p) \rho_t(\vec{r}_t) v_d(\vec{s}) + \int \int d\vec{r}_p d\vec{r}_t \rho_p(\vec{r}_p) \rho_t(\vec{r}_t) v_{ex}(\vec{s}), \quad (8)$$

where U_D and U_{EX} direct and exchange folding potentials, respectively.

There are two approaches for the exchange parts of the interactions; these are zero-range (ZR) [15, 16] or finite-range (FR) [17] knock-on exchange interactions. The ZR approaches given in Eqs. (3) and (6), where $\varepsilon = E/a_p$ is the projectile's incident energy per nucleon in the laboratory frame, are widely used in the literature due to their simplicity in calculations. One needs only to put the ZR interactions in 3 or Eq. (6) to the exchange part of Eq. (8) to obtain the exchange part of the DF potential (U_{EX}). The depths of the ZR interactions are defined by $J_{ex}(E)$. Determination of $J_{ex}(E)$ is empirically done; the detailed information can be found in Refs. [15, 16, 11].

As is pointed out by Khoa [17], the exchange interaction, in general, must be nonlocal [18]. Thus, the exact numerical calculation of exchange interaction can become too complicated. A plain wave [19] approximation for the relative motion of nucleons can overcome this complication and lead to an equivalent local potential. The plain wave given in Ref. [3] is

$$\chi(\vec{R} + \vec{s}) \approx \exp\left(\frac{i\vec{K}(\vec{R}) \cdot \vec{s}}{M}\right) \chi(\vec{R}), \quad (9)$$

where $M = a_p a_t / (a_p + a_t)$ is the recoil factor (or reduced mass), while a_p and a_t are the mass numbers of the projectile and target nuclei, respectively. And $\vec{K}(\vec{R})$ is the local momentum of the relative motion given by [18]

$$K^2(\vec{R}) = \frac{2mM}{\hbar^2} \left[E_{c.m.} - U_D(\vec{R}) - U_{EX}(\vec{R}) - U_C(\vec{R}) \right], \quad (10)$$

where $E_{c.m.}$ is relative energy in the center-of-mass system, m is the nucleon mass, and U_C is the Coulomb potential. Then, local exchange potential will take the form of [17, 18, 20, 21, 22, 23]:

$$U_{EX}(\vec{R}) = \int \int d\vec{r}_p d\vec{r}_t \rho_p(\vec{r}_p, \vec{r}_p + \vec{s}) \rho_t(\vec{r}_t, \vec{r}_t - \vec{s}) v_{ex}(\vec{s}) \exp\left(\frac{i\vec{K}(\vec{R}) \cdot \vec{s}}{M}\right), \quad (11)$$

where $\rho_p(\vec{r}_p, \vec{r}_p + \vec{s})$ and $\rho_t(\vec{r}_t, \vec{r}_t - \vec{s})$ are one-body density matrices [22, 23, 24] of the projectile and target nucleons. This local potential becomes an FR exchange potential when $v_{ex}(\vec{s})$ is chosen as one of the FR interactions in Eqs. (4) or (7) (M3Y-Reid/Paris-FR). One should realize that the exchange part of Eq. (8) needs to be replaced by Eq. (11) for the FR exchange potential.

The next step in the exchange potential (Eq. (8)) is the calculation of density matrices. Although the matrices can be obtained from single-particle wave functions [18], Khoa [17] has chosen a realistic local approximation from Ref. [25]:

$$\rho_{p,t}(\vec{r}, \vec{r} \pm \vec{s}) \approx \rho_{p,t} \left(\vec{r} \pm \frac{\vec{s}}{2} \right) \hat{j}_1 \left(k_{F_{p,t}} \left(\vec{r} \pm \frac{\vec{s}}{2} \right) s \right), \quad (12)$$

where $\hat{j}_1(x) = 3(\sin x - x \cos x)/x^3$. k_F is the average local Fermi momentum from Refs. [25, 26, 27, 28]:

$$k_F(\vec{r}) = \left\{ \left[\frac{3}{2} \pi^2 \rho(\vec{r}) \right]^{2/3} + C_S \frac{5}{3} \frac{[\nabla \rho(\vec{r})]^2}{\rho^2(\vec{r})} + \frac{5}{36} \frac{\nabla^2 \rho(\vec{r})}{\rho(\vec{r})} \right\}^{1/2}, \quad (13)$$

where ρ is the nuclear matter densities of the projectile or the target and C_S is the strength of the Weizsäcker term, representing the surface contribution to the kinetic energy density [27]. The strength term is usually $C_S \approx \frac{1}{36}$ in the literature, but Khoa *et al.* [27] have taken it as $C_S \approx \frac{1}{4}$ for the given reasons in their work. The default value is $C_S \approx \frac{1}{36}$ in BiFold, but the user has the option to change the value.

After this point, the FR exchange potential will have the following form [17]:

$$U_{EX}(\vec{R}) = 4\pi \int_0^\infty v_{EX}(s) s^2 ds \int f_p(\vec{r}, \vec{s}) f_t(\vec{r} - \vec{R}, \vec{s}) j_0(K(\vec{R})s/M) d\vec{r} \quad (14)$$

where $f_{p,t}(\vec{r}, \vec{s}) = \rho_{p,t}(\vec{r}) \hat{j}_1(k_{F,p,t}(\vec{r})s)$ and $j_0(x) = \sin x/x$. Now, the exchange potential with Fourier transforms in spherical coordinates will take the form [1, 17]:

$$U_{EX}(R) = 4\pi \int_0^\infty G(R, s) j_0(K(R)s/M) v_{EX}(s) s^2 ds, \quad (15)$$

where

$$G(R, s) = \frac{1}{2\pi^2} \int_0^\infty f_p(q, s) f_t(q, s) j_0(qR) q^2 dq, \quad (16)$$

$$f_{p,t}(q, s) = 4\pi \int_0^\infty f_{p,t}(r, s) j_0(qr) r^2 dr. \quad (17)$$

Finally, it is necessary to solve a self-consistency problem to obtain the exchange part (Eq. (11)) of the double folded potential (Eq. (8)) at each radial point. Since the exchange potential (Eq. (11)) contains the local momentum of the relative motion (Eq. (10)) and $\vec{K}(\vec{R})$ depends on the total double folded potential, this problem can be solved exactly by an iterative method given in Refs. [27, 29, 22, 23].

2.3. Effective density-dependent NN interactions

The effective density-dependent NN interaction is proposed [2, 27, 28, 30] in the following form for both direct (v_d) and exchange (v_{ex}) parts;

$$v_{d,ex}(\rho, E, \vec{s}) = g(E) F_{d,ex}(\rho) v_{d,ex}(\vec{s}) \quad (18)$$

where ρ is the overlapping density of the nuclear medium of both nuclei. $g(E)$ is the weak intrinsic energy dependence proposed by Khoa *et al.* [31]. The density-dependent folding potential with an FR exchange part can be calculated by replacing this new form with $v_d(\vec{s})$ in Eq. (8) and with $v_{ex}(\vec{s})$ in Eq. (11). In the case of a ZR exchange part [32], it can be calculated by using the new form for both $v_d(\vec{s})$ and $v_{ex}(\vec{s})$ in Eq. (8).

The overlapping density for the direct part and the ZR exchange part of the folded potential has been approximated in most of the folding potential calculations [2, 33, 34, 27, 9, 35, 29, 32] as

$$\rho = \rho_p(\vec{r}_p) + \rho_t(\vec{r}_t), \quad (19)$$

Table 1: BiFold can calculate double folding potentials for the interactions marked with “√” where ZR and FR stand for zero-range and finite-range exchange interactions, respectively. The × stands for not supported or non existing interactions. The nuclear incompressibility values (K [MeV]) are only exist for finite range versions of the interactions [35, 29].

Interaction names	ZR	FR	C	α	β [fm ³]	γ [fm ³ⁿ]	n	K [MeV]	Refs.	
DDM3Y	Reid	✓	×	$C(E)$	$\alpha(E)$	$\beta(E)$	0.0	0	[2, 34]	
DDM3Y1	Reid	✓	✓	0.2845	3.6391	2.9605	0.0	0	171	[31, 27, 9, 3]
DDM3Y1	Paris	✓	✓	0.2963	3.7231	3.7384	0.0	0	176	[9, 35, 3]
BDM3Y0	Reid	×	×	1.3827	0.0	0.0	1.1135	2/3	232	[31]
BDM3Y1		✓	✓	1.2253	0.0	0.0	1.5124	1	232	
BDM3Y2	Reid	✓	✓	1.0678	0.0	0.0	5.1069	2	354	[31, 27, 9, 3]
BDM3Y3		✓	✓	1.0153	0.0	0.0	21.073	3	475	
BDM3Y1		✓	✓	1.2521	0.0	0.0	1.7452	1	270	
BDM3Y2	Paris	✓	✓	1.0664	0.0	0.0	6.0296	2	418	[9, 35, 3]
BDM3Y3		✓	✓	1.0045	0.0	0.0	25.115	3	566	
CDM3Y1		✓	✓	0.3429	3.0232	3.5512	0.5	1	188	
CDM3Y2		✓	✓	0.3346	3.0357	3.0685	1.0	1	204	
CDM3Y3	Paris	✓	✓	0.2985	3.4528	2.6388	1.5	1	217	[29, 3]
CDM3Y4		✓	✓	0.3052	3.2998	2.3180	2.0	1	228	
CDM3Y5		✓	✓	0.2728	3.7367	1.8294	3.0	1	241	
CDM3Y6		✓	✓	0.2658	3.8033	1.4099	4.0	1	252	
M3Y	Reid	✓	✓	usual density-independent M3Y					[1, 17, 32]	
M3Y	Paris	✓	✓							

since it permits the separation of variables in the integrals of Eqs. (8) and (11). The overlapping density for the FR exchange part of the folded potential has been assumed [2, 33, 34, 27, 9, 35, 29, 32] as

$$\rho = \rho_p(\vec{r}_p + \frac{\vec{s}}{2}) + \rho_t(\vec{r}_t - \frac{\vec{s}}{2}). \quad (20)$$

The code can calculate double folding potentials for the interactions marked with a “√” in Table 1. The density dependence of these interactions is defined by $F(\rho)$ in Eq. (18). Different versions of 18 are proposed in the Refs. [2, 31, 9, 29]. In a more recent study by Khoa *et al.* [3], these different versions of $F(\rho)$ merged into one formula;

$$F(\rho) = C[1 + \alpha \exp(-\beta\rho) - \gamma\rho^n]. \quad (21)$$

The parameters of this formula are given in Table 1 other than the original DDM3Y [2] since its parameters are energy-dependent. The values of these energy-dependent parameters can be obtained from the Refs. [2, 34].

The final part of the density-dependent NN interaction (Eq. (18)) is $g(E)$. It is $g(E) = 1$ for the original DDM3Y [2] since $g(E)$ does not exist for this interaction. For the remaining density-dependent interactions in Table 1, $g(E) \approx 1 - \kappa\varepsilon$, where $\kappa = 0.002$ and $\kappa = 0.003$ for the M3Y-Reid and M3Y-Paris types of interactions, respectively, and $\varepsilon = E/a_p$ is energy (in MeV) per nucleon.

3. The code

The file structure of BiFold code given is in Fig. 2 on the left. The bold ones are directories, and the rest are Python files in the given file structure. The two sub-directories in the **bifold** direc-

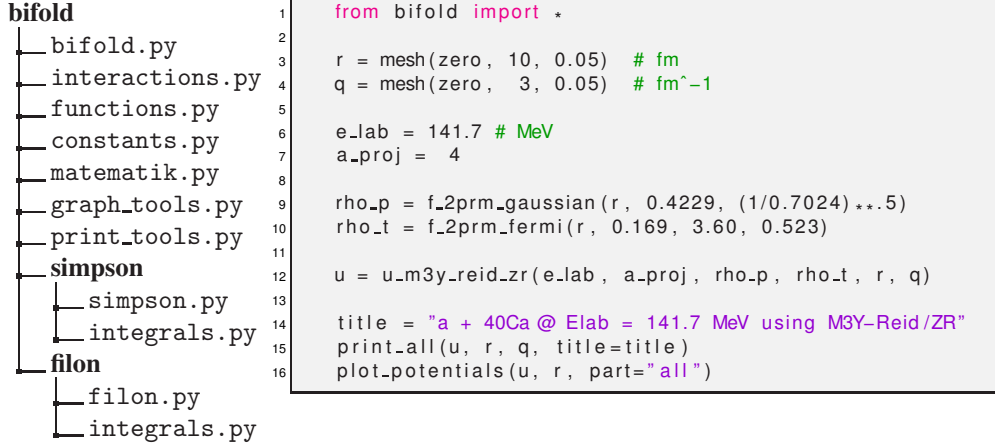


Figure 2: The file tree structure of BiFold code is on the left. The bold ones are directories, and the rest are Python files. And an example Python file to calculate a double folding potential for an $\alpha+^{40}\text{Ca}$ elastic scattering on the right.

tory (**simpson** and **filon**) have the same structures other than the integration methods. ‘*bifold.py*’ file calls ‘*simpson.py*’ file since the Simpson integration method is the default integration method of BiFold. Both ‘*simpson.py*’ and ‘*filon.py*’ have the functions with the names starts-with ‘*u_*’ since the symbols of the double folding potentials are U_{DF} or U_D or U_{EX} in Eq. (8). Therefore, ‘*simpson.py*’ (‘*filon.py*’) is the main part of the code where the calculation of the double folding integrals takes place through ‘*integrals.py*’. Table 2 shows the names of these functions that correspond to the calculation of double folding potential types. Table 2 also lists the Python functions of the ‘*interactions.py*’ file for the computation of the effective NN interactions in Eqs. (2) through (7). The ‘*functions.py*’ file contains Python functions for nuclear matter densities and effective NN interactions. Table 3 shows the mathematical representations of the densities and interactions versus Python representations. The ‘*matematik.py*’ contains the spherical Bessel functions, numerical derivation functions, and other mathematical tools. The ‘*constants.py*’ is for all the necessary physical and mathematical constants. The other two files (‘*graph_tools.py*’ and ‘*print_tools.py*’) are for drawing and printing the results.

Table 2: The presented names are the Python functions in BiFold to calculate the effective NN interactions and the doubling potentials. The \times stands for not supported or non existing potentials/interactions.

Interaction names		‘ <i>simpson.py</i> ’/ ‘ <i>filon.py</i> ’		‘ <i>interactions.py</i> ’		
		U_{DF} with ZR	U_{DF} with FR	$v_d(\vec{s})$	ZR: $v_{ex}(\vec{s})$	FR: $v_{ex}(\vec{s})$
DDM3Y	Reid	u_ddm3y_reid_zr	\times	v_m3y_reid_d	v_m3y_reid_ex_zr	\times
DDM3Y1						
BDM3Yn; n = 1, 2, 3	Reid	u_xdm3yn_zr	u_xdm3yn_fr	v_m3y_reid_d	v_m3y_reid_ex_zr	v_m3y_reid_ex_fr
DDM3Y1						
BDM3Yn; n = 1, 2, 3	Paris	u_xdm3yn_zr	u_xdm3yn_fr	v_m3y_paris_d	v_m3y_paris_ex_zr	v_m3y_paris_ex_fr
CDM3Yn; n = 1...6						
M3Y	Reid	u_m3y_reid_zr	u_xdm3yn_fr	v_m3y_reid_d	v_m3y_reid_ex_zr	v_m3y_reid_ex_fr
M3Y	Paris	u_m3y_paris_zr		v_m3y_paris_d	v_m3y_paris_ex_zr	v_m3y_paris_ex_fr

An example Python file for calculating a density-independent double potential using M3Y-Reid NN interaction with the ZR exchange part (see Eqs. (2) and (3)) for an $\alpha+^{40}\text{Ca}$ elastic

Table 3: The presented names are the Python functions in BiFold to calculate the nuclear matter densities or, if necessary, to write a new type of interaction or to calculate phenomenological potentials.

Python function	Math formula	Python function	Math formula
f_exp_decay(r, V0, a)	$V_0 e^{-ar}$	f_sog(r, Ris, Qis, RP, Ze)	$\sum_i A_i \left\{ e^{-[(r-R_i)/\gamma]^2} + e^{-[(r+R_i)/\gamma]^2} \right\}$ [36]
f_yukawa(r, V0, a, b)	$V_0 e^{-ar}/br$	f_dirac_delta(r, V0)	$V_0 \delta(r)$
f_2prm_fermi(r, V0, R, a)	$V_0 \frac{1}{1+e^{-\frac{r-R}{a}}}$	f_external(r, external_data) ¹	reads from a local file
f_3prm_fermi(r, V0, w, R, a)	$V_0 \frac{1+w^2}{1+e^{-\frac{r-R}{a}}}$	f_internet(r, url) ¹	reads a file from a given url
f_2prm_gaussian(r, V0, a)	$V_0 e^{-(r/a)^2}$	f_ripl(r, Z, A) ¹	HFB14 densities from RIPL [37, 38, 39, 40]
f_3prm_gaussian(r, V0, w, a)	$V_0 (1 + wr^2) e^{-(r/a)^2}$		https://www-nds.iaea.org/RIPL

¹ These functions create Python arrays using data from local or remote files. These arrays contain interpolated values to match the given r array defined by the $mesh(r_{min}, r_{max}, dr)$ function.

scattering is on the right side of Fig. 2. And the results of the calculation are shown in Figs. 3 and 4. One may agree that the code is easy to understand. The first line of the Python code imports BiFold since it is a Python package. On the third and fourth lines, the *mesh* functions defines the numerical integration grids for $r = zero$ fm to $r = 10$ fm with 0.05 fm steps and $q = zero$ fm⁻¹ to $r = 3$ fm⁻¹ with 0.05 fm⁻¹ steps where $zero = 1 \times 10^{-10}$. The sixth and seventh lines are the laboratory energy (*e_Lab*) and the atomic mass number (*a_proj*) of the projectile (α - particle), respectively. The ninth and tenth lines are the nuclear matter densities of the projectile (*rho_p*) and the target (*rho_t*) nuclei, respectively. The twelfth line is the double folding calculation in Eq. (8) for M3Y-Reid NN interaction with the ZR exchange part (see Eqs. (2) and (3)). The rest of the file is optional if one needs to print (Fig. 3) the calculation information and draw (Fig. 4) the potentials versus radial distance between the two nuclei. This code is a simple example of how to use BiFold to calculate a double-folded potential. The related GitHub (<https://github.com/mkarakoc/BiFold>) page has the BiFold code, a more detailed user guide, and more examples.

a + 40Ca @ Elab = 141.7 MeV using M3Y-Reid/ZR							
density/interaction	L	norm	renorm	vol2	vol4	msr	
-----total-----							
u_R : u_m3y_reid_zr	0	None	1.000	-59536.370	-982867.456	16.509	
-----direct-----							
u_R : u_direct	0	None	1.000	-23281.699	-486747.684	20.907	
rho_p : f_2prm_gaussian	0	None	1.000	4.000	8.543	2.136	
rho_t : f_2prm_fermi	0	None	1.000	39.908	461.090	11.554	
vnn : f_yukawa	0	None	1.000	1570.558	588.970	0.375	
vnn : f_yukawa	0	None	1.000	-1716.459	-1647.805	0.960	
-----exchange-----							
u_R : u_exchange_zr	0	None	1.000	-36254.670	-496119.772	13.684	
rho_p : f_2prm_gaussian	0	None	1.000	4.000	8.543	2.136	
rho_t : f_2prm_fermi	0	None	1.000	39.908	461.090	11.554	
vnn : f_dirac_delta	0	None	1.000	-227.114	0.000	0.000	
R	u_R	R	u_R	R	u_R	R	u_R
0.000	-224.563778558	2.500	-157.142066726	5.000	-33.591208578	7.500	-1.294809340
0.050	-224.538322266	2.550	-154.527402817	5.050	-32.017487683	7.550	-1.195282003
0.100	-224.461928239	2.600	-151.883273803	5.100	-30.494524998	7.600	-1.102914652
0.150	-224.334521330	2.650	-149.211853484	5.150	-29.022094646	7.650	-1.017241399
...							
...							
2.300	-167.264509196	4.800	-40.395194787	7.300	-1.774804137	9.800	-0.024215666
2.350	-164.788335884	4.850	-38.617900517	7.350	-1.641422081	9.850	-0.022007393
2.400	-162.274567943	4.900	-36.891404224	7.400	-1.517343866	9.900	-0.019983036
2.450	-159.725143549	4.950	-35.215829117	7.450	-1.401989622	9.950	-0.018129460

Figure 3: It is the output of the double folding potential calculation for the $\alpha+^{40}\text{Ca}$ elastic scattering.

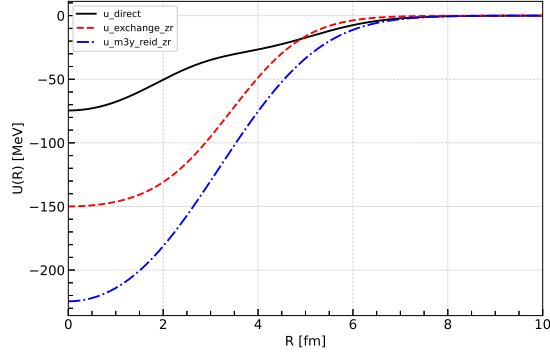


Figure 4: It is the double folding potential [dash-dot] with direct [solid] and exchange [dash] parts for the $\alpha+^{40}\text{Ca}$ elastic scattering.

The output of the BiFold calculation shown in Fig. 3 gives individual information about the potentials and the functions used in the calculations. This individual information from left to right contains a Python dictionary key, name of the function/potential, multi-polarity (L), normalization (norm) and re-normalization (renorm), volume integrals (vol2 and vol4), and mean square radii (msr). The output also contains printout of the calculated potential U_R versus radial distance R between two nuclei.

The dictionary keys *func_i*, *func_r* and *func_q* store the information about the function, numeric values of the function at every point defined by $mesh(r_{min}, r_{max}, dr)$, and numeric values of the function's Fourier transform at every point defined by $mesh(q_{min}, q_{max}, dq)$, respectively. The output does not list these keys. The keys *total*, *direct* and *exchange* are to reach total, direct and exchange individual parts of the calculations under the previous keys. And *u_R*, *rho_p*, *rho_t*, and *vm* keys store information about every individual part under the previous keys. Finally, one can reach the information tabulated in the output by using *L*, *norm*, *renorm*, *vol2*, *vol4* and *msr* keys. For example, using *func_i*, *direct* and *rho_p* keys in the given order will produce the following output about the density of the projectile nucleus in the example code in Fig. 2:

```

1 input : u['func_i']['direct']['rho_p']
2 output: [{'name': 'f_2prm_gaussian', 'L': 0, 'norm': None, 'renorm': 1.0,
3          'vol2': 4.000237160, 'vol4': 8.542647693, 'msr': 2.135535308}]

```

The following formula defines the volume integrals for all radial dependent functions and potentials,

$$vol(n+2) = renorm 4\pi \int f(r)r^{n+2}dr. \quad (22)$$

If the value of *norm* is *None*, then *renorm* = 1, otherwise if *norm* is a real number, then *renorm* is,

$$renorm = norm \left[4\pi \int f(r)r^{n+2}dr \right]^{-1}. \quad (23)$$

The mean square radii (msr) of all radial dependent functions and potentials are $\langle r^2 \rangle = vol4/vol2$.

4. Test cases

This section compares BiFold computations to three examples to demonstrate the code's reliability. The first one is an analytical calculation, and the second one is a numerical calculation using DFPOT [7]. And the work of Khoa *et al.* [35] is the last one. One can assume that the examples are reasonably accurate since the first example is an exact solution to the double folding integrals, the second example is a published code used and tested many times in the literature, and the final one is a reliable published work. Therefore, these examples are reference calculations to use in the following formula,

$$\xi^2 = \frac{1}{N} \sum_i^N \left(\frac{U_A(R_i) - U_B(R_i)}{U_A(R_i) + U_B(R_i)} \right)^2. \quad (24)$$

This formula defines a mean relative error (mre) [8] for comparing BiFold calculations with reference calculations where U_A and U_B are the reference and the present double folding potentials with the radial distance R_i , respectively. It is better if ξ^2 is getting closer to zero, as it will mean that the results of both computations are getting more consistent. The results of the mre calculations are in Table 4, and the details of the test cases are in the following sections.

Table 4: The mean relative errors, defined by Eq. (24), are given for the three test cases. The cases are compared with BiFold's calculations using both Simpson's and Filon's integration.

Integration method of BiFold	ξ^2	Analytical		DFPOT	Khoa <i>et al.</i> [35]
		$q_{max} = 3 \text{ fm}^{-1}$	$q_{max} = 10 \text{ fm}^{-1}$		
Simpson	total	2.16×10^{-3}	6.66×10^{-8}	1.31×10^{-7}	6.58×10^{-5}
	direct	1.84×10^2	1.19×10^{-7}	8.10×10^{-5}	6.65×10^{-3}
	exchange	1.22×10^0	5.87×10^{-6}	1.40×10^{-6}	2.48×10^{-5}
Filon	total	2.16×10^{-3}	6.64×10^{-8}	1.31×10^{-7}	6.57×10^{-5}
	direct	1.84×10^2	1.16×10^{-7}	8.13×10^{-5}	6.65×10^{-3}
	exchange	1.22×10^0	5.87×10^{-6}	1.40×10^{-6}	2.48×10^{-5}

4.1. BiFold vs. analytical calculation

In this case, $\alpha + \alpha$ scattering with projectile energy 50 MeV in the laboratory system is in consideration. Satchler and Love [1] suggested a Gaussian shaped nuclear matter distribution for an $\alpha -$ particle is

$$\rho(r) = 0.4229 e^{-0.7024r^2} \text{ fm}^{-3}, \quad (25)$$

with a mean square radius $\langle r^2 \rangle = 2.1355 \text{ fm}^2$. A new nuclear matter distribution for the $\alpha -$ particle is

$$\rho(r) = 2.12 e^{-2.3705r} \text{ fm}^{-3}, \quad (26)$$

proposed using the msr value since the previous one does not allow to obtain an analytical solution. Therefore, the reason for choosing this distribution is to obtain an exact analytical double-folded potential since the density-independent NN effective interaction (M3Y-Reid, Eq. (2) also has a similar mathematical form. Then this is easily achieved by using the Fourier transform

techniques as usual [1] for the double folding integral given in Eq. (8), but this time with an analytical integration. Thus, the analytical double-folded potential with both direct and ZR exchange NN interactions included is

$$U(R) = \frac{1}{R} 2747 (e^{-4R} - 31323.3246 e^{-2.5R} - 10.729866914 e^{-2.3705R} \times [R^3 - 24.345R^2 + 377.89705R - 2919.17177]). \quad (27)$$

Both computations agree very well, as supported by the ξ^2 values in Table 4 and shown in Fig. 5a. The ξ^2 values are almost the same for both integration methods. There is a caveat to be careful of about this case. The effective NN interaction and the new nuclear matter distribution slowly go to zero when r goes to infinity, contrary to the Gaussian-shaped density in Eq. (25). This leads to the problem shown in Fig. 5b, where $q_{max} = 3 \text{ fm}^{-1}$ is not enough to obtain a numerically accurate solution. Therefore it was necessary to raise q_{max} to 10 fm^{-1} in this case while this value of q_{max} is usually enough most of the time, as mentioned in Ref. [7]. This problem illustrates it is better to make a consistency check by raising the value of q_{max} till the calculation reaches a saturation point where the potential does not change anymore.

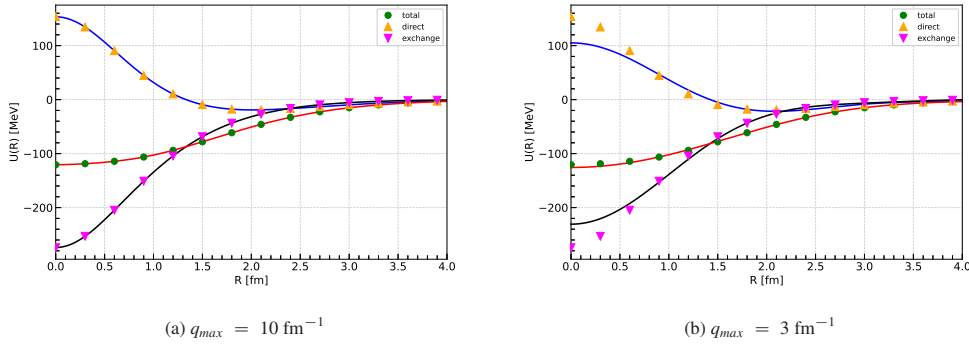


Figure 5: The full circles, up triangles, and down triangles are the calculations of the total, direct and exchange parts of the analytically calculated double folding potentials, respectively. The solid lines are the computations using BiFold.

4.2. BiFold vs. DFPOT

This test case compares the two codes for an $\alpha + {}^{40}\text{Ca}$ elastic scattering system where the energy of the α projectile is 141.7 MeV in the laboratory system. The effective NN interaction is for both codes is the density-independent M3Y-Paris with the ZR exchange part given in Eqs. (5) and (6). BiFold can perform the calculation for this case by changing ‘*u_m3y_reid_zr*’ to ‘*u_m3y_paris_zr*’ in the twelfth line of Python code shown in Fig. 2.

The nuclear matter density for α – particle is in Eq. (25), and the density [34] of ${}^{40}\text{Ca}$ is

$$\rho(r) = 0.169 \left[1 + \exp\left(\frac{r - 3.60}{0.523}\right) \right]^{-1} \text{ fm}^{-3}, \quad (28)$$

with a msr value of $\langle r^2 \rangle = 11.553 \text{ fm}^2$. As seen in Fig. 6, the computations of both codes are in very well agreement with each other, and the ξ^2 values in Table 4 also support the claim.

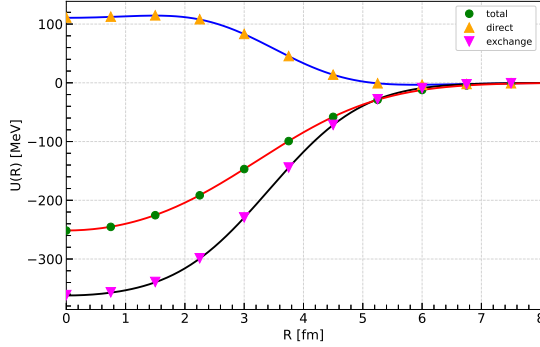


Figure 6: The full circles, up triangles, and down triangles are the calculations of the total, direct and exchange parts of the double folding potentials using DF POT [7], respectively. The solid lines are the computations using BiFold.

4.3. BiFold vs. Khoa *et al.*'s calculation

The $^{16}\text{O}+^{16}\text{O}$ elastic scattering system at several incident energies was studied by Khoa *et al.* [35] using various density-dependent M3Y-Paris-based NN interactions. The case chosen for the comparison is the one at 250 MeV incident energy. And the effective NN interaction used for the double folding potential is the BDM3Y1-Paris NN interaction with the FR exchange part. The calculations of Khoa *et al.* [35] were obtained by digitizing the related figure in the reference with the help of the programs Inkscape [41] and Engauge Digitizer [42].

The nuclear matter density of the ^{16}O nuclei with the msr value $\langle r^2 \rangle = 6.625 \text{ fm}^2$ [34, 35] is

$$\rho(r) = 0.181 \left[1 + \exp\left(\frac{r - 2.525}{0.45}\right) \right]^{-1} \text{ fm}^{-3}. \quad (29)$$

Since BDM3Y1 is a density-dependent NN interaction, the double folding integral in Eq. (11) has to be solved to obtain the potentials in Fig. 7. This integral contains the Coulomb potential between the two nuclei through the local momentum $\vec{K}(\vec{R})$ of the relative motion. The Coulomb potential modeled for uniformly charged spherical nuclei is

$$U_C(R) = z_p z_t \frac{e^2}{4\pi\epsilon_0} \begin{cases} \frac{1}{R} & (R \geq R_C) \\ \frac{1}{2R_c} \left[3 - \left(\frac{R}{R_c}\right)^2 \right] & (R \leq R_C) \end{cases} \quad (30)$$

used in the calculations where z_p, z_t are proton numbers of the projectile and the target, respectively. The Coulomb radius is $R_c = 1.405 \left(a_p^{1/3} + a_t^{1/3} \right) \text{ fm}$.

As can be seen from the ξ^2 values in Table 4 and the potentials in Fig. 7, BiFold is also consistent with the final reference work. It is important to note here that the comparison is made till 5.6 fm in this case since the resolution of the digitized figure [35] was not enough to recover the data with enough precision.

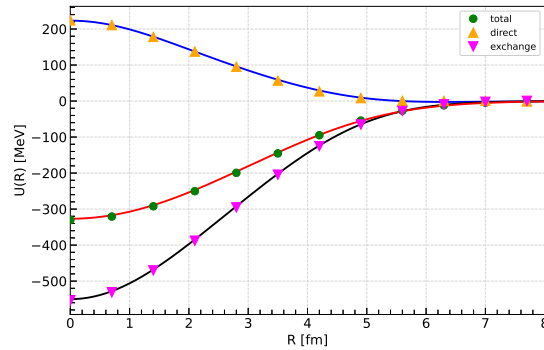


Figure 7: The full circles, up triangles, and down triangles are the calculations of the total, direct and exchange parts of the double folding potentials from Khoa *et al.* [35], respectively. The solid lines are the computations using BiFold.

Declaration of competing interest

The author declares that he has no known competing financial interests or personal relationships that could have appeared to influence the work reported in this paper.

Acknowledgements

The author would like to thank Prof. Dr. O. Bayrak for stimulating discussions and useful comments on the manuscript.

References

- [1] G. Satchler, W. Love, Folding model potentials from realistic interactions for heavy-ion scattering, *Physics Reports* 55 (3) (1979) 183–254. doi:[https://doi.org/10.1016/0370-1573\(79\)90081-4](https://doi.org/10.1016/0370-1573(79)90081-4). URL <https://www.sciencedirect.com/science/article/pii/0370157379900814>
- [2] A. Kobos, B. Brown, P. Hodgson, G. Satchler, A. Budzanowski, Folding model analysis of α -particle elastic scattering with a semirealistic density-dependent potential, *Nuclear Physics A* 384 (1) (1982) 65–87. doi:[https://doi.org/10.1016/0375-9474\(82\)90305-0](https://doi.org/10.1016/0375-9474(82)90305-0). URL <https://www.sciencedirect.com/science/article/pii/0375947482903050>
- [3] D. T. Khoa, W. von Oertzen, H. G. Bohlen, S. Ohkubo, Nuclear rainbow scattering and nucleus–nucleus potential, *Journal of Physics G: Nuclear and Particle Physics* 34 (3) (2007) R111–R164. doi:[10.1088/0954-3899/34/3/r01](https://doi.org/10.1088/0954-3899/34/3/r01). URL <https://doi.org/10.1088/0954-3899/34/3/r01>
- [4] M. Karakoc, I. Boztosun, α - α double folding cluster potential description of the $^{12}\text{C} + ^{24}\text{Mg}$ system, *Phys. Rev. C* 73 (2006) 047601. doi:[10.1103/PhysRevC.73.047601](https://doi.org/10.1103/PhysRevC.73.047601). URL <https://link.aps.org/doi/10.1103/PhysRevC.73.047601>
- [5] G. R. Satchler, *Direct nuclear reactions* (Jan 1983).
- [6] D. A. Goldberg, The alpha-nucleus interaction : proceedings of the 2nd louvain-cracow seminar, held in louvain-la-neuve, june 1978, Louvain-la-Neuve : Institut Interuniversitaire des Sciences Nucléaires Université de Louvain, Louvain-la-Neuve, 1978.
- [7] J. Cook, Dfpot - a program for the calculation of double folded potentials, *Computer Physics Communications* 25 (2) (1982) 125–139. doi:[https://doi.org/10.1016/0010-4655\(82\)90029-7](https://doi.org/10.1016/0010-4655(82)90029-7). URL <https://www.sciencedirect.com/science/article/pii/0010465582900297>
- [8] I. Gontchar, M. Chushnyakova, A c-code for the double folding interaction potential of two spherical nuclei, *Computer Physics Communications* 181 (1) (2010) 168–182. doi:<https://doi.org/10.1016/j.cpc.2009.09.007>. URL <https://www.sciencedirect.com/science/article/pii/S0010465509002860>

- [9] D. T. Khoa, W. von Oertzen, Refractive alpha-nucleus scattering: a probe for the incompressibility of cold nuclear matter, *Physics Letters B* 342 (1) (1995) 6–12. doi:[https://doi.org/10.1016/0370-2693\(94\)01393-Q](https://doi.org/10.1016/0370-2693(94)01393-Q).
URL <https://www.sciencedirect.com/science/article/pii/037026939401393Q>
- [10] G. Bertsch, J. Borysowicz, H. McManus, W. Love, Interactions for inelastic scattering derived from realistic potentials, *Nuclear Physics A* 284 (3) (1977) 399–419. doi:[https://doi.org/10.1016/0375-9474\(77\)90392-X](https://doi.org/10.1016/0375-9474(77)90392-X).
URL <https://www.sciencedirect.com/science/article/pii/037594747790392X>
- [11] M. Brandan, G. Satchler, The interaction between light heavy-ions and what it tells us, *Physics Reports* 285 (4) (1997) 143–243. doi:[https://doi.org/10.1016/S0370-1573\(96\)00048-8](https://doi.org/10.1016/S0370-1573(96)00048-8).
URL <https://www.sciencedirect.com/science/article/pii/S0370157396000488>
- [12] R. V. Reid, Local phenomenological nucleon-nucleon potentials, *Annals of Physics* 50 (3) (1968) 411–448. doi:[https://doi.org/10.1016/0003-4916\(68\)90126-7](https://doi.org/10.1016/0003-4916(68)90126-7).
URL <https://www.sciencedirect.com/science/article/pii/0003491668901267>
- [13] M. Lacombe, B. Loiseau, J. M. Richard, R. V. Mau, J. Côté, P. Pirès, R. de Tourreil, Parametrization of the paris $n - n$ potential, *Phys. Rev. C* 21 (1980) 861–873. doi:10.1103/PhysRevC.21.861.
URL <https://link.aps.org/doi/10.1103/PhysRevC.21.861>
- [14] N. Anantaraman, H. Toki, G. Bertsch, An effective interaction for inelastic scattering derived from the paris potential, *Nuclear Physics A* 398 (2) (1983) 269–278. doi:[https://doi.org/10.1016/0375-9474\(83\)90487-6](https://doi.org/10.1016/0375-9474(83)90487-6).
URL <https://www.sciencedirect.com/science/article/pii/0375947483904876>
- [15] W. Love, L. Owen, Exchange effects from realistic interactions in the reformulated optical model, *Nuclear Physics A* 239 (1) (1975) 74–82. doi:[https://doi.org/10.1016/0375-9474\(75\)91133-1](https://doi.org/10.1016/0375-9474(75)91133-1).
URL <https://www.sciencedirect.com/science/article/pii/0375947475911331>
- [16] Satchler, Love, Comment on “Elastic scattering of 318 MeV ${}^6\text{Li}$ from ${}^{12}\text{C}$ and ${}^{28}\text{Si}$: Unique phenomenological and folding-model potentials” and the Physical review. C, *Nuclear physics* 49 4 (1994) 2254–2257. doi:<https://doi.org/10.1103/PhysRevC.49.2254>.
URL <https://journals.aps.org/prc/abstract/10.1103/PhysRevC.49.2254>
- [17] Dao Tien Khoa, Exchange effects in nuclear rainbow scattering, *Nuclear Physics A* 484 (2) (1988) 376–396. doi:[https://doi.org/10.1016/0375-9474\(88\)90077-2](https://doi.org/10.1016/0375-9474(88)90077-2).
URL <https://www.sciencedirect.com/science/article/pii/0375947488900772>
- [18] B. Sinha, The optical potential and nuclear structure, *Physics Reports* 20 (1) (1975) 1–57. doi:[https://doi.org/10.1016/0370-1573\(75\)90011-3](https://doi.org/10.1016/0370-1573(75)90011-3).
URL <https://www.sciencedirect.com/science/article/pii/0370157375900113>
- [19] B. Sinha, S. A. Moszkowski, The nucleus-nucleus interaction potential using density-dependent delta interaction, *Physics Letters B* 81 (3) (1979) 289–294. doi:[https://doi.org/10.1016/0370-2693\(79\)90337-X](https://doi.org/10.1016/0370-2693(79)90337-X).
URL <https://www.sciencedirect.com/science/article/pii/037026937990337X>
- [20] F. Brieva, J. Rook, Nucleon-nucleus optical model potential: (i). nuclear matter approach, *Nuclear Physics A* 291 (2) (1977) 299–316. doi:[https://doi.org/10.1016/0375-9474\(77\)90322-0](https://doi.org/10.1016/0375-9474(77)90322-0).
URL <https://www.sciencedirect.com/science/article/pii/0375947477903220>
- [21] F. Brieva, J. Rook, Nucleon-nucleus optical model potential: (ii). finite nuclei, *Nuclear Physics A* 291 (2) (1977) 317–341. doi:[https://doi.org/10.1016/0375-9474\(77\)90323-2](https://doi.org/10.1016/0375-9474(77)90323-2).
URL <https://www.sciencedirect.com/science/article/pii/0375947477903232>
- [22] A. Chaudhuri, D. Basu, B. Sinha, An α -nucleus optical potential using a realistic effective interaction, *Nuclear Physics A* 439 (3) (1985) 415–426. doi:[https://doi.org/10.1016/0375-9474\(85\)90419-1](https://doi.org/10.1016/0375-9474(85)90419-1).
URL <https://www.sciencedirect.com/science/article/pii/0375947485904191>
- [23] A. Chaudhuri, B. Sinha, A microscopic optical model analysis of heavy ion elastic scattering data using the realistic nn interaction, *Nuclear Physics A* 455 (1) (1986) 169–178. doi:[https://doi.org/10.1016/0375-9474\(86\)90350-7](https://doi.org/10.1016/0375-9474(86)90350-7).
URL <https://www.sciencedirect.com/science/article/pii/0375947486903507>
- [24] S. K. Gupta, B. Sinha, Intrinsic density and energy dependence: Exchange effects in alpha-nucleus scattering, *Phys. Rev. C* 30 (1984) 1093–1095. doi:10.1103/PhysRevC.30.1093.
URL <https://link.aps.org/doi/10.1103/PhysRevC.30.1093>
- [25] X. Campi, A. Bouyssy, A simple approximation for the nuclear density matrix, *Physics Letters B* 73 (3) (1978) 263–266. doi:[https://doi.org/10.1016/0370-2693\(78\)90509-9](https://doi.org/10.1016/0370-2693(78)90509-9).
URL <https://www.sciencedirect.com/science/article/pii/0370269378905099>
- [26] P. Ring, P. Schuck, *The nuclear many-body problem*, Springer-Verlag, New York, 1980, p. 542.
- [27] D. T. Khoa, W. von Oertzen, H. G. Bohlen, Double-folding model for heavy-ion optical potential: Revised and applied to study ${}^{12}\text{C}$ and ${}^{16}\text{O}$ elastic scattering, *Phys. Rev. C* 49 (1994) 1652–1668. doi:10.1103/PhysRevC.49.1652.
URL <https://link.aps.org/doi/10.1103/PhysRevC.49.1652>
- [28] D. T. Khoa, α -nucleus optical potential in the double-folding model, *Phys. Rev. C* 63 (2001) 034007. doi:10.1103/PhysRevC.63.034007.
URL <https://link.aps.org/doi/10.1103/PhysRevC.63.034007>
- [29] D. T. Khoa, G. R. Satchler, W. von Oertzen, Nuclear incompressibility and density dependent NN interactions in the folding model for nucleus-nucleus scattering, *Phys. Rev. C* 63 (2001) 034007. doi:10.1103/PhysRevC.63.034007.

- Phys. Rev. C 56 (1997) 954–969. doi:10.1103/PhysRevC.56.954.
 URL <https://link.aps.org/doi/10.1103/PhysRevC.56.954>
- [30] D. T. Khoa, G. Satchler, Generalized folding model for elastic and inelastic nucleus–nucleus scattering using realistic density dependent nucleon–nucleon interaction, Nuclear Physics A 668 (1) (2000) 3–41. doi:[https://doi.org/10.1016/S0375-9474\(99\)00680-6](https://doi.org/10.1016/S0375-9474(99)00680-6).
 URL <https://www.sciencedirect.com/science/article/pii/S0375947499006806>
- [31] D. T. Khoa, W. von Oertzen, A nuclear matter study using the density dependent m3y interaction, Physics Letters B 304 (1) (1993) 8–16. doi:[https://doi.org/10.1016/0370-2693\(93\)91391-Y](https://doi.org/10.1016/0370-2693(93)91391-Y).
 URL <https://www.sciencedirect.com/science/article/pii/037026939391391Y>
- [32] K. Hagino, T. Takehi, N. Takigawa, No-recoil approximation to the knock-on exchange potential in the double folding model for heavy-ion collision, Physical Review C 74 (2006) 037601. doi:<https://doi.org/10.1103/PhysRevC.74.037601>.
 URL <https://journals.aps.org/prc/abstract/10.1103/PhysRevC.74.037601>
- [33] A. Kobos, B. Brown, R. Lindsay, G. Satchler, Folding-model analysis of elastic and inelastic α -particle scattering using a density-dependent force, Nuclear Physics A 425 (2) (1984) 205–232. doi:[https://doi.org/10.1016/0375-9474\(84\)90073-3](https://doi.org/10.1016/0375-9474(84)90073-3).
 URL <https://www.sciencedirect.com/science/article/pii/0375947484900733>
- [34] M.-A. Farid, G. Satchler, A density-dependent interaction in the folding model for heavy-ion potentials, Nuclear Physics A 438 (2) (1985) 525–535. doi:[https://doi.org/10.1016/0375-9474\(85\)90391-4](https://doi.org/10.1016/0375-9474(85)90391-4).
 URL <https://www.sciencedirect.com/science/article/pii/0375947485903914>
- [35] D. T. Khoa, W. v. Oertzen, H. G. Bohlen, G. Bartnitzky, H. Clement, Y. Sugiyama, B. Gebauer, A. N. Ostrowski, T. Wilpert, M. Wilpert, C. Langner, Equation of state for cold nuclear matter from refractive $^{16}\text{O} + ^{16}\text{O}$ elastic scattering, Phys. Rev. Lett. 74 (1995) 34–37. doi:10.1103/PhysRevLett.74.34.
 URL <https://link.aps.org/doi/10.1103/PhysRevLett.74.34>
- [36] H. De Vries, C. De Vries, C. De Vries, Nuclear charge-density-distribution parameters from elastic electron scattering, Atomic Data and Nuclear Data Tables 36 (3) (1987) 495–536. doi:[https://doi.org/10.1016/0092-640X\(87\)90013-1](https://doi.org/10.1016/0092-640X(87)90013-1).
 URL <https://www.sciencedirect.com/science/article/pii/0092640X87900131>
- [37] R. Capote, M. Herman, P. Obložinský, P. Young, S. Goriely, T. Belgya, A. Ignatyuk, A. Konig, S. Hilaire, V. Plujko, M. Avrigeanu, O. Bersillon, M. Chadwick, T. Fukahori, Z. Ge, Y. Han, S. Kailas, J. Kopecky, V. Maslov, G. Reffo, M. Sin, E. Soukhovitskii, P. Talou, Ripl – reference input parameter library for calculation of nuclear reactions and nuclear data evaluations, Nuclear Data Sheets 110 (12) (2009) 3107–3214, special Issue on Nuclear Reaction Data. doi:<https://doi.org/10.1016/j.nds.2009.10.004>.
 URL <https://www.sciencedirect.com/science/article/pii/S0090375209000994>
- [38] S. Goriely, M. Samyn, J. M. Pearson, Further explorations of skyrme-hartree-fock-bogoliubov mass formulas. vii. simultaneous fits to masses and fission barriers, Phys. Rev. C 75 (2007) 064312. doi:10.1103/PhysRevC.75.064312.
 URL <https://link.aps.org/doi/10.1103/PhysRevC.75.064312>
- [39] G. Audi, A. Wapstra, C. Thibault, The ame2003 atomic mass evaluation: (ii). tables, graphs and references, Nuclear Physics A 729 (1) (2003) 337–676, the 2003 NUBASE and Atomic Mass Evaluations. doi:<https://doi.org/10.1016/j.nuclphysa.2003.11.003>.
 URL <https://www.sciencedirect.com/science/article/pii/S0375947403018098>
- [40] I. Angeli, A consistent set of nuclear rms charge radii: properties of the radius surface $r(n,z)$, Atomic Data and Nuclear Data Tables 87 (2) (2004) 185–206. doi:<https://doi.org/10.1016/j.adt.2004.04.002>.
 URL <https://www.sciencedirect.com/science/article/pii/S0092640X04000166>
- [41] M. Owens, M. Jeanmougin, C. Rogers, T. Gould, T. Bah, J. Andler, Inkscape (Last Accessed September 20, 2022).
 URL <https://inkscape.org/>
- [42] M. Mitchell, B. Muftakhidinov, T. Winchen, Engauge digitizer software (Last Accessed September 20, 2022).
 URL <http://markummitchell.github.io/engauge-digitizer/>